

Thermal expansion at a metal surface: A study of Mg(0001) and Be(10 $\bar{1}$ 0)Ismail,^{1,2} Ph. Hofmann,³ A. P. Baddorf,² and E. W. Plummer^{1,2}¹*Department of Physics and Astronomy, The University of Tennessee, Knoxville, Tennessee 37996-1200*²*Solid State Division, Oak Ridge National Laboratory, Oak Ridge, Tennessee 37831-6057*³*Institute for Storage Ring Facilities, Universities of Aarhus, DK-8000 Aarhus C, Denmark*

(Received 23 May 2002; published 20 December 2002)

Quantitative low-energy electron diffraction current-voltage measurements have been utilized to determine the thermal expansion of the Mg(0001) and Be(10 $\bar{1}$ 0) surfaces. The close-packed Mg(0001) surface exhibits a small thermal expansion while the more open Be(10 $\bar{1}$ 0) surface has a dramatic thermal contraction in the first interlayer spacing, accompanied by an expansion in the second interlayer spacing. A comparison of this data with all other measurements of the low-temperature thermal expansion reveals a quite striking difference for open surfaces of different metals. Significant negative thermal contraction at the surface occurs only on open faces of light mass metals. A simple force constant model indicates that this behavior correlates with the ratio of thermal motion parallel and perpendicular to the surface.

DOI: 10.1103/PhysRevB.66.245414

PACS number(s): 68.35.Ja, 61.14.Hg, 65.40.De

I. INTRODUCTION

When a crystal is divided to form two surfaces the symmetry is broken and there is a redistribution of the electrons and atoms to lower the energy. One obvious result is a new static structure at the surface. In the simplest cases this results in a one-dimensional change in the interlayer spacing near the surface. More dramatic rearrangements result in a two-dimensional reconstruction. In almost all cases of metal surfaces the experimental static structure (low temperature) and first-principles calculations agree quite well. The physics behind the interlayer relaxation of metal surfaces is well understood.¹⁻³ Smoluchowski¹ proposed that at the surface, charge smoothing would occur to lower the kinetic energy of the electrons. Charge moves from above a surface atom to the hollow between them. This charge smoothing is more dramatic on open faces and explains the lower work functions exhibited by open surfaces.¹ Finnis and Heine,² using simple electrostatic arguments, demonstrated that this lead to a reduction in the first interlayer spacing at the surface. This picture predicts larger contraction on the more open surfaces and little contraction on the close-packed ones. On the close-packed faces there should be little Smoluchowski smoothing and small outward relaxation has been predicted as a result of the electron density tail that extends into the vacuum attracting the ion cores away from the solid.³ This picture is consistent with what has been called the “universal curve”^{4,5} that relates the change in the first interlayer spacing Δd_{12} to the area of the surface unit cell A_s . When these two parameters are properly normalized to the volume per atom in the bulk, V_o , all of the data and first-principles calculation seem to fall in a region centered on a straight line given by $(\Delta d_{12}/V_o^{1/3}) = -0.1149 + 0.1296/A_o$. A_o is the area of the surface unit cell (A_s) properly normalized to the volume of the bulk unit cell, $A_o = A_s/V_o^{2/3}$. The static structure at a surface has been developed to the stage where a detailed picture of multilayer relaxation exists.⁶

Obviously, while the general trend in static relaxation can be explained by the simple-picture described above, at some level the details of the bonding of the metal become

important.⁷ d -bonded metals are different from either noble metals or simple sp -bonded metals, but the simple picture presented above explains the general trend observed in static relaxation. Nonetheless, as Feibelman pointed out, there is a discrepancy between the calculated and measured first interlayer relaxation for a series of reactive transition metal close-packed surfaces [Ti(0001), Zr(0001), Mo(110), Rh(0001), and W(110)].⁸ Most of the data used in this comparison are old and Feibelman suggested that hydrogen contamination could be the cause of the disagreement. However, a recent surface x-ray diffraction study of Ru(0001) concluded that the discrepancy between experiment and theory for the first interlayer spacing change Δd_{12} is not a consequence of hydrogen contamination.⁹ Another possibility, relevant to the discussions in this paper, concerns thermal expansion. All of the structures were determined at room temperature while the calculations were for $T=0$ K. There is no general understanding of thermal expansion at a surface, so it is difficult to extract the $T=0$ K structure from data taken at elevated temperatures.

In stark contrast to the static structure at a surface, where theory and experiment generally agree and there is a zero-order accepted explanation, an understanding of the dynamical behavior of a surface waits to be developed. In fact, the observed thermal behavior at a surface has been described as violating “common sense.”¹⁰ All that this statement means is that our intuition or common sense has not been properly developed. Some close-packed surfaces exhibit anomalously large thermal expansion¹¹ in the first interlayer spacing, while a more open surface displays thermal contraction in the first interlayer spacing^{12,13} accompanied by thermal expansion of the second interlayer spacing or even oscillatory thermal expansion.¹³ Yet this is not universal, since Al(110) displays a thermal contraction in d_{12} while Cu(110) and Ag(110)^{14,15} display a positive thermal expansion in d_{12} . On the theory front there is mixed success, with examples where first-principles theory and experiment agree^{13,16,17} or dramatically disagree.^{18,19} Even for the success stories the theory has not presented us with an insight into the origin of the thermal behavior of a metal surface. A quotation from Phil Anderson’s 1978 Nobel lecture eloquently describes the

situation: “After all, the perfect computation simply reproduces Nature. It does not explain her.”

The origin of the complexity in understanding thermal expansion is that at a finite temperature the position of the atoms is determined by minimizing the free energy. The free energy contains the details of the electronic and lattice excitations at a temperature T . Two recent calculations have begun to shed light on the origin, what appears to be a violation of “common sense” with respect to the thermal properties of open metal surfaces.^{10,16} An impressive *ab initio* molecular dynamics (MD) study of the Al(110) surface¹⁶ has reproduced the measured thermal contraction in d_{12} .^{12,20} The origin of the thermal contraction is the anomalously large vibrational amplitude of the second layer atoms perpendicular to the surface. Narasimhan explored the vibrational properties of Cu(110), Ag(110), and Al(110) by performing *ab initio* calculations of the surface force constants for a structurally relaxed surface.¹⁰ The most striking result was the large enhancement in the first to third layer force constants and a reduction of the surface in-plane force constants. This reduces the out-of-plane vibrations and enhances the in-plane vibrations. The strong first to third layer force constants coupled with an almost harmonic potential-energy curve for perpendicular displacement of the planes with respect to each other makes d_{13} rigid and allows d_{12} and d_{23} to respond to increasing temperature in opposite ways. Two very important insights in surface thermal expansion were presented in this paper.

(1) Thermal expansion or contraction occurs without anharmonicity in the interplanar potential.

(2) The force constants in the surface are not redistributed for an unrelaxed surface.

These two observations illustrate why our intuition has not progressed very far. One cannot think in terms of anharmonicity in this region of broken symmetry and one cannot start with a model of a bulk-truncated surface. It is imperative to first understand what the static reconstruction has done to the force constants at the surface and then how these new force constants affect the surface phonons.

It should also be pointed out that it is not clear what features of either a calculation or an experiment need to be examined to understand the microscopic nature of surface thermal properties. For example, the MD calculation for Al(110) discovered a soft channel for vibrations of the second layer atoms perpendicular to the surface.¹⁶ It is strange that this anomalous channel for surface vibrations was never recognized in either the experimental (He scattering²¹) or theoretical (first principles²² and molecular dynamics²³) investigations of the surface phonon spectra on Al(110).

Given the state of confusion associated with thermal expansion at a metal surface it seems clear that more data are needed which might lead to the formulation of empirical rules that can be explored theoretically, leading to a general zero-order explanation. The temperature dependent interlayer spacing $d_{ij}(T) = d_{ij}(0) + \beta_{ij}T$ (where T is temperature and β_{ij} is the coefficient of the linear expansion of the separation between the i th and j th planes), has been measured for the close-packed Mg(0001) surface ($1/A_o = 0.913$), and the open Be(10 $\bar{1}$ 0) surface ($1/A_o = 0.490$). The surface thermal-

expansion coefficient of the first interlayer spacing given by $\alpha_{12} = (1/d_{12})(\partial d_{12}/\partial T)$ or $\alpha_{12} = \beta_{12}/d_{12}(0)$ was determined from low-energy electron diffraction (LEED) I - V measurements to be $+4.5 \times 10^{-5} \text{ K}^{-1}$ for Mg(0001) and $-23.8 \times 10^{-5} \text{ K}^{-1}$ for Be(10 $\bar{1}$ 0). For comparison, the thermal contraction at the surface of Be is 20 times that of the bulk thermal expansion, and Mg is $+1.5$ the bulk value. The values of α_{12} for these two surfaces will be compared with all other measurements of the low-temperature thermal expansion at metal surfaces. This comparison reveals a quite striking difference for open surfaces of different metals. Negative thermal expansion at the surface seems to occur only on open faces of light mass metals. A simple force constant model indicates that this behavior correlates with the ratio of thermal motion parallel and perpendicular to the surface.

The experimental details and results will be presented in Sec. II. Section III will describe the experimental comparison for thermal expansion at a metal surface. Section IV will present speculation on the origin of the trends observed in the surface thermal expansion coefficients, and Sec. V contains our conclusion.

II. EXPERIMENTAL DETAILS AND RESULTS

A. The Be(10 $\bar{1}$ 0) surface

The experiments were performed using a standard ultra-high vacuum chamber with a base pressure of 7×10^{-11} Torr. A clean Be(10 $\bar{1}$ 0) sample with the surface area of $5 \times 5 \text{ mm}^2$ (square) and thickness of 3 mm was prepared by repeated sputter-anneal cycles. Sputtering was done with Ne^+ at a kinetic energy of 1 kV, and a sample temperature of 550 K. The subsequent annealing was at 700 K. The cleanness of sample was monitored with high-resolution electron energy loss spectroscopy (HREELS). A sharp (1×1) LEED pattern was observed in the temperature range studied (110 to 500 K) indicating that the Be(10 $\bar{1}$ 0) surface does not reconstruct. LEED intensities of the integer order diffracted beams as a function of incident electron energy were recorded using a video LEED system with 0.5 eV increments at normal incidence for sample temperatures 110, 300, and 500 K. Normal incidence was determined by adjusting the position of the sample until the $I(V)$ curves of the equivalent beams were identical, i.e., the Pendry R factor (R_p) (Ref. 24) between the equivalent beams is less than 0.1. All equivalent beams were averaged and normalized to the beam current. Eight inequivalent beams $\{(10), (01), (11), (02), (20), (12), (03), \text{ and } (13)\}$ were recorded with the total energy range of $\Delta E = 1900 \text{ eV}$ for temperature $T = 110 \text{ K}$. For $T = 300 \text{ K}$ there were eight inequivalent beams $\{(10), (01), (11), (02), (20), (12), (03), \text{ and } (13)\}$ with the total energy range of $\Delta E = 1400 \text{ eV}$. At $T = 500 \text{ K}$ only five inequivalent beams $\{(10), (01), (11), (02), \text{ and } (12)\}$ were recorded, with the total energy range of $\Delta E = 950 \text{ eV}$. The reduction in the data set with increasing temperature is the consequence of Debye-Waller attenuation at higher beam energies.

Analysis of the LEED I - V spectra was carried out using standard multiple scattering algorithms combined with the

TABLE I. Geometric parameters with respect to the bulk extracted from the best-fit spectra to the LEED I - V data for Be(10 $\bar{1}$ 0) as a function of temperature, where $\Delta d_{ij}(T)=[d_{ij}(T)-d_{ij}^{\text{bulk}}(T)]/d_{ij}^{\text{bulk}}(T)$.

	$T=0$ K (extrapolated)	$T=110$ K	$T=300$ K	$T=500$ K	β_{ij} ($\text{\AA}/\text{K}$)
Δd_{12} (%)	-27	-23.5(\pm 3.0)	-26.7(\pm 3.4)	-30.8(\pm 3.8)	-12.3×10^{-5}
Δd_{23} (%)	+5.4	+6.6(\pm 1.5)	+7.1(\pm 1.7)	+9.6(\pm 1.9)	$+11.8 \times 10^{-5}$
Δd_{34} (%)	-13.6	-13.4(\pm 3.4)	-15.1(\pm 3.8)	-14.2(\pm 4.5)	-0.7×10^{-5}
Δd_{45} (%)	+1.5	+3.0(\pm 1.8)	+3.3(\pm 1.9)	+6.5(\pm 2.2)	$+13.5 \times 10^{-5}$
d_{12}^{bulk} (\AA)	0.6579	0.6589	0.6598	0.6618	0.789×10^{-5}
d_{23}^{bulk} (\AA)	1.3358	1.3178	1.3196	1.3262	1.60×10^{-5}
LEED nonstructural parameters					
$\langle u \rangle_1$ (\AA)		0.166	0.196	0.244	
$\langle u \rangle_2$ (\AA)		0.126	0.173	0.213	
$\langle u \rangle_{\text{bulk}}$ (\AA)		0.114	0.148	0.180	
C (eV)		-4.25	-4.75	-4.50	
V_{or} (eV)		8.05	8.57	8.53	
R_p		0.176	0.152	0.163	

automated tensor-LEED programs of Barbieri and Van Hove.²⁵ Fourteen atomic phase shifts for Be were employed in our calculations, which we derived using a muffin-tin potential. Electron attenuation was included by the energy-dependent imaginary part of the optical potential V_{oi} represented by the equation $V_{\text{oi}}=C\{E/(7.35+V_{\text{or}})\}^{1/3}$ eV where E is the incident electron energy, C a parameter. The real part of the optical potential (V_{or}) is a constant optimized during the search. The thermal vibration of the atoms was introduced via a Debye-Waller factor, where the Debye temperature was converted into isotropic mean-square displacements $\langle u^2 \rangle$. The first $\langle u^2 \rangle_1$ and second $\langle u^2 \rangle_2$ layer vibrational amplitudes were used as parameters to fit the experimental data. The third and deeper layers were forced to have the same bulk value $\langle u^2 \rangle_B$. Best fit to measured spectra was determined by Pendry R factor (R_p) and the error bar was calculated as defined by Pendry.²⁴ Temperature dependence of the bulk lattice constants was obtained from x-ray data.²⁶ Calculated intensities are compared to the experimental spectra to search a minimum R_p factor by using the automated search algorithm to obtain the surface structures. No in-plane relaxation was considered in the calculations.

The temperature dependent measurements of the surface structure of Be(10 $\bar{1}$ 0) are tabulated in Table I. The agreement between the experimental spectra and calculated multiple scattering, using the parameters in Table I, is excellent, reflected in the R_p factors. Previous structural analysis of this surface has shown that the surface is terminated with the bulk short interlayer spacing,⁵ called d_{12}^{bulk} in Table I. The comparison between the experimental and calculated spectra is shown in Fig. 1. Figure 2 plots the temperature dependence of d_{12} , d_{23} , d_{34} , d_{bulk} for both the short and long bulk interplanar spacing. There is both oscillatory interplanar relaxation and oscillatory thermal expansion.

The temperature-dependent data can be extrapolated linearly to $T=0$ K yielding the values for the interplanar spacing presented in Table I for $T=0$ K. To facilitate a comparison to other materials Table I displays the percent change in

d_{ij} with respect to the bulk value d_{ij}^{bulk} , where $\Delta d_{ij}(T)=[d_{ij}(T)-d_{ij}^{\text{bulk}}(T)]/d_{ij}^{\text{bulk}}(T)$. As the temperature increases, the first (third) interlayer spacing contracts, while the second (fourth) interlayer spacing expands. Since the interlayer spacing is assumed to be a linear function of temperature for temperature below premelting regime, the experimental data were fitted with a straight line to determine β_{ij} (defined in the Introduction). The experimental values of β_{ij} are shown in Table I. The surface thermal expansion coefficient between the interlayer spacing is given by $\alpha_{ij}=\beta_{ij}/d_{ij}(0)$. The data presented in Fig. 2 for Be(10 $\bar{1}$ 0) yield a surface thermal expansion coefficient of $-23.8(\pm 9.0) \times 10^{-5}$ 1/K in the first interlayer, $+9.1(\pm 5.4) \times 10^{-5}$ 1/K in the second interlayer, $-1.0(\pm 9.8) \times 10^{-5}$ 1/K in the third interlayer, and $+10.2(\pm 7.2) \times 10^{-5}$ 1/K in the fourth interlayer. For comparison, the value of the bulk thermal expansion is $\approx 1.2 \times 10^{-5}$ 1/K. The thermal data are in good agreement with calculations within the quasiharmonic calculations.²⁷

B. The Mg(0001) surface

The same ultrahigh vacuum chamber and LEED I - V apparatus used for Be(10 $\bar{1}$ 0) experiments were used for Mg(0001) experiments. A clean Mg(0001) sample with the surface area of 50 mm² (circle) and thickness of 3 mm was prepared by sputtering with Ne⁺ at a kinetic energy of 1 kV and sample temperature 400 K, and subsequently annealing at 450 K. Repeating this procedure results a sharp (1 \times 1) LEED pattern and a clean surface as defined by HREELS.

The Mg(0001) surface does not reconstruct in the temperature range investigated, $T=130$ K to $T=400$ K. The (1 \times 1) LEED pattern showed a sixfold symmetry, indicating an averaging over the two terminations (A and B) of the threefold symmetry of ideal hcp(0001). Intensities of the integer order diffracted beams as a function of incident electron energy were recorded with 0.5 eV increments at normal incidence for sample temperatures 130, 300, and 400 K. All equivalent beams were averaged and normalized to the beam

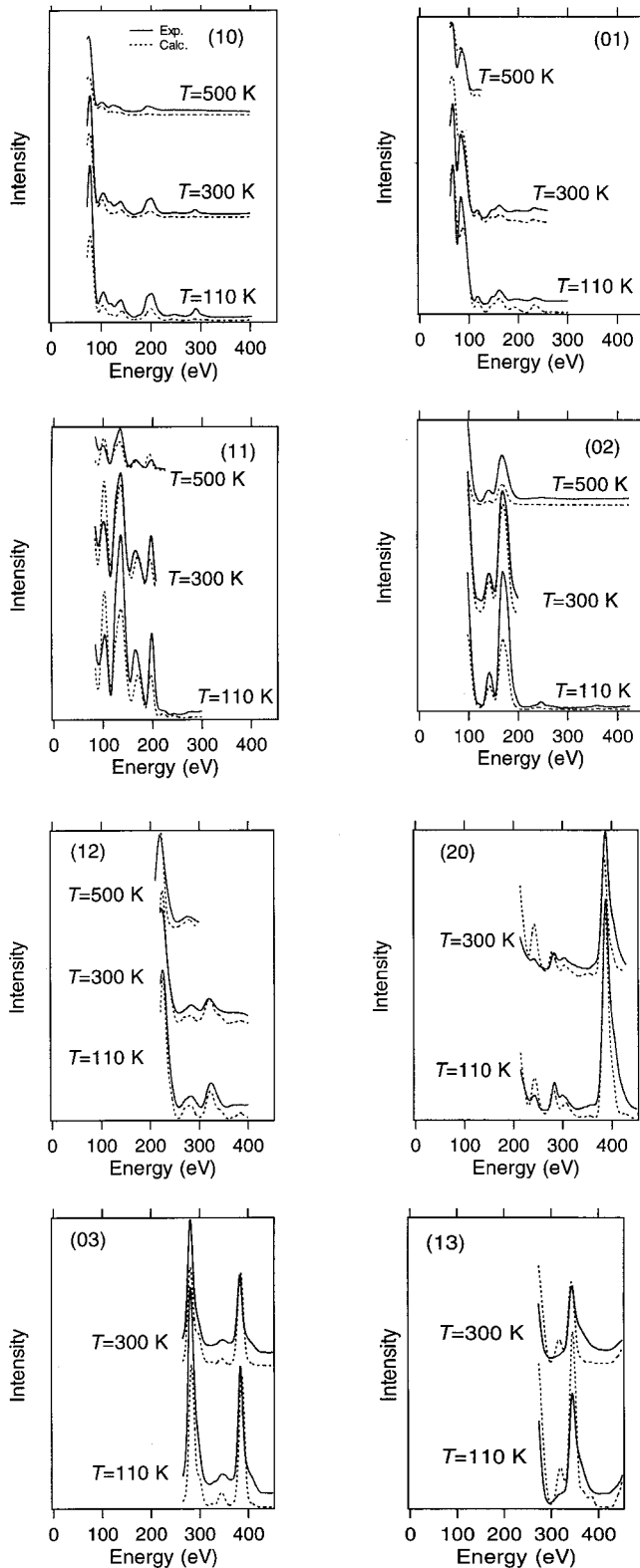


FIG. 1. Comparison of LEED data for Be($10\bar{1}0$) with multiple scattering calculations for the structure presented in Table I.

current. The data set consisted of four inequivalent beams $\{(01), (11), (02), \text{and } (21)\}$ with the total energy range of $\Delta E = 1425$ eV for a temperature $T = 130$ K; three inequivalent beams $\{(01), (11), \text{and } (02)\}$ with the total energy range

of $\Delta E = 740$ eV for a temperature $T = 300$ K; and two inequivalent beams $\{(01) \text{ and } (11)\}$ with the total energy of $\Delta E = 560$ eV for a temperature $T = 400$ K. As in the case of Be($10\bar{1}0$), the reduction in the data set with increasing temperature is the consequence of Debye-Waller attenuation at higher beam energies.

The surface structure was obtained using the same procedure described for Be($10\bar{1}0$). Fourteen atomic phase shifts for Mg were employed in our calculations, which we derived using a muffin-tin potential approximation. Electron attenuation was included by the energy-dependent imaginary part of the optical potential V_{oi} that is similar to the case of Be($10\bar{1}0$).

Comparison between the experimental and best-fit calculated spectra is shown in Fig. 3. The agreement between the experimental spectra and the multiple scattering calculation is excellent, given the structural and nonstructural parameters shown in Table II. The fit is reflected in the Rp factors presented in the table. The smaller Rp factor at higher temperature is related to the reduction in the data set with increasing temperature. Figure 4 is a plot of the interplanar spacing at the surface and in the bulk as a function of temperature. The straight line fits to the data are used to determine the values of β_{ij} s (see Table II). The extrapolation of the data to $T = 0$ K is presented in Table II. Within experimental error the relaxation in the deeper layers (d_{23} and d_{34}) are the same as in the bulk. The data at $T = 130$ K are in excellent agreement with the previous experimental study at $T = 100$ K,²⁸ and the extrapolation to $T = 0$ K is in excellent agreement with first-principles calculations.²⁹ The surface thermal expansion coefficient α_{12} for the first interlayer

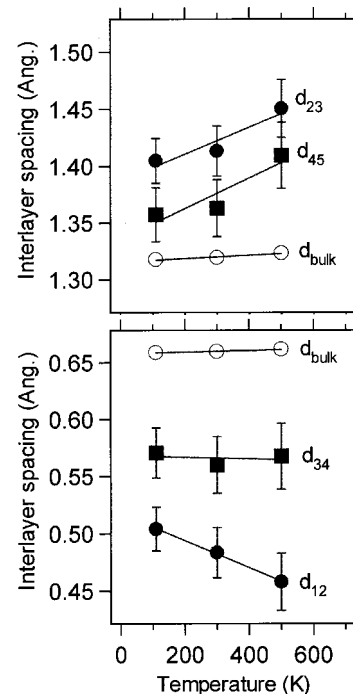


FIG. 2. A plot of d_{ij} as a function of temperature for Be($10\bar{1}0$) obtained for the LEED data. The lines are the best fit to the experimental data.

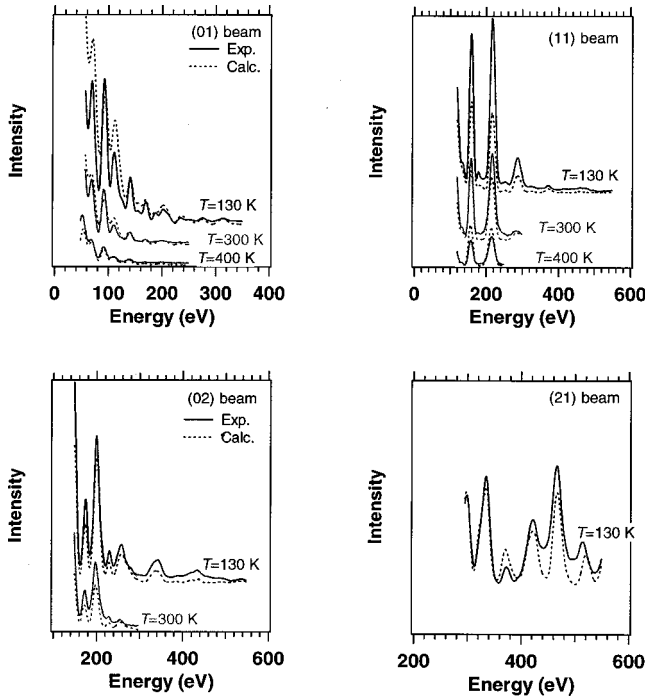


FIG. 3. Comparison of LEED data for Mg(0001) with multiple scattering calculations for the structure presented in Table II.

spacing d_{12} is found to be $+4.5(\pm 2.8) \times 10^{-5}$ 1/K, where the bulk thermal expansion coefficient of Mg is 2.5×10^{-5} 1/K.

III. GENERAL TRENDS IN d_{ij} AND α_{ij}

The results presented in the preceding section for the surface thermal properties of the close-packed Mg(0001) and open Be(10 $\bar{1}$ 0) surfaces are similar to data in the literature for other sp -bonded metal surfaces. Thermal contraction is observed for the first interplanar spacing on open surfaces such as Mg(10 $\bar{1}$ 0) (Ref. 13) and Al(110) (Refs. 12 and 20), and thermal expansion is common on close-packed surfaces

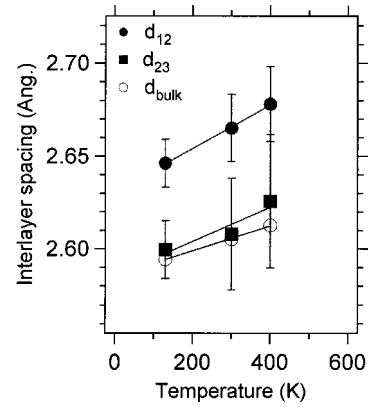


FIG. 4. A plot of d_{ij} as a function of temperature for Mg(0001) obtained from the LEED data. The lines are the best fit to the data.

such as Be(0001) (Ref. 11) and Al(111) (Ref. 30). In contrast, most of the transition or noble metals exhibit small thermal expansion for all faces studied. To illustrate this point, Figure 5(a) displays all of the reported data for α_{12} as a function of the inverse of the normalized surface area $1/A_o$. This figure seems to indicate that there is something fundamentally different between the surface thermal expansion behavior of open surface of sp -bonded metals compared to transition or noble metals. But the calculations by Narasimhan¹⁰ for the fcc(110) surface of Cu, Ag, and Al indicated that on all three metals there was an appreciable strengthening of the first to third layer force constant resulting from the static relaxation in d_{12} and d_{23} . She predicted that this would lead to rigidity in the lattice spacing of d_{13} as a function of temperature. Figure 5(b) dramatically illustrates her point by plotting α_{13} as a function of the inverse of the surface area ($1/A_o$). Amazingly, α_{13} is almost independent of $1/A_o$ and the identity of the metal. The real question now is: why does the second atomic plane behave the way it does?

It is important to remember that in the Narasimhan's calculation the dramatic changes in the force constants only occur for a relaxed surface. Therefore the properties of the d_{ij} s as a function of $1/A_o$ and the nature of the bonding in

TABLE II. Geometric parameters extracted from best fit to LEED I - V data of Mg(0001) as a function of temperature. $\langle u \rangle_i$ is the root-mean-square displacement of the i th layer, where $\Delta d_{ij}(T) = [d_{ij}(T) - d_{ij}^{\text{bulk}}(T)]/d_{ij}^{\text{bulk}}(T)$.

	$T=0$ K (extrapolated)	$T=130$ K	$T=300$ K	$T=400$ K	β_{ij} ($\text{\AA}/\text{K}$)
Δd_{12} (%)	+1.76	+1.96(± 0.5)	+2.34(± 0.7)	+2.48(± 1.1)	+11.8 $\times 10^{-5}$
Δd_{23} (%)	+0.0	+0.2(± 0.6)	+0.1(± 1.1)	+0.5(± 1.4)	+9.2 $\times 10^{-5}$
Δd_{34} (%)	+0.0	+0.0(± 0.9)	+0.1(± 1.3)	+0.2(± 1.5)	+6.5 $\times 10^{-5}$
d (\AA)	2.5855	2.5944	2.6053	2.6127	+6.46 $\times 10^{-5}$
LEED nonstructural parameters					
$\langle u \rangle_1$ (\AA)		0.195	0.285	0.327	
$\langle u \rangle_2$ (\AA)		0.140	0.197	0.226	
$\langle u \rangle_{\text{bulk}}$ (\AA)		0.113	0.152	0.173	
C (eV)		-5.0	-5.0	-5.0	
V_{or} (eV)		3.02	3.24	3.44	
R_P		0.13	0.11	0.10	

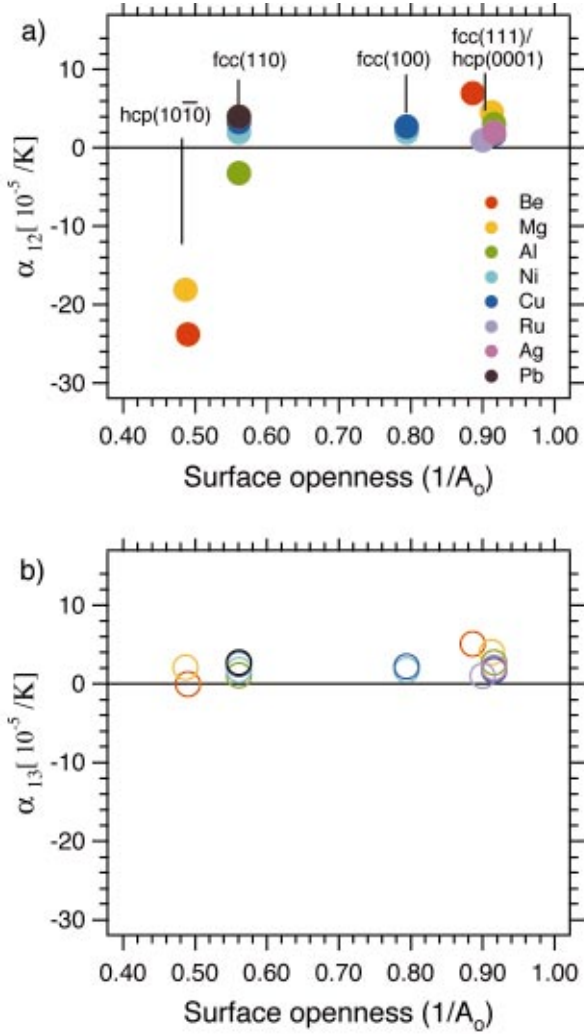


FIG. 5. (Color) Measured surface thermal expansion coefficients, α_{12} (a) for the first interlayer spacing and α_{23} , (b) for the second interlayer spacing as a function of the openness of surface ($1/A_o$). The references for data points are: Be(0001) (Ref. 11), Mg(0001) (this study), Al(111) (Ref. 30), Ag(111) (Ref. 31), Cu(111) (Ref. 32), Ni(111) (Ref. 33), Cu(100) (Ref. 34), Ni(100) (Ref. 35), Pb(110) (Ref. 36), Cu(110) (Ref. 14), Ag(110) (Ref. 15), Ni(110) (Ref. 37), Al(110) (Refs. 12 and 20), Mg(10 $\bar{1}0$) (Ref. 13), Be(10 $\bar{1}0$) (this study). The color code is shown in (a).

the host metal are very important and might shed light on the nature of the thermal properties. Figure 6(a) plots Δd_{12} (circles) and Δd_{23} (squares) as a function of $1/A_o$ for the same materials displayed in Fig. 5. There are also data for the static relaxation for the more open surfaces displayed in this figure, i.e., the Al(331) surface, and the (210) surfaces of Cu and Al. For surfaces where $1/A_o$ is larger than 0.4, in general, d_{23} responds in an opposite way to d_{12} . When Δd_{12} is very negative then Δd_{23} is positive. However, for more open face where $1/A_o$ is smaller than 0.4 [i.e., fcc(210), fcc(331)], both Δd_{12} and Δd_{23} are negative. As was the case with the thermal expansion coefficient, the plot of Δd_{13} as a function of $1/A_o$ shown in Fig. 6(b) is very illuminating. Δd_{13} has the same dependence on the openness of the surface as Δd_{12} . Evidently, Narasimhan's picture, developed

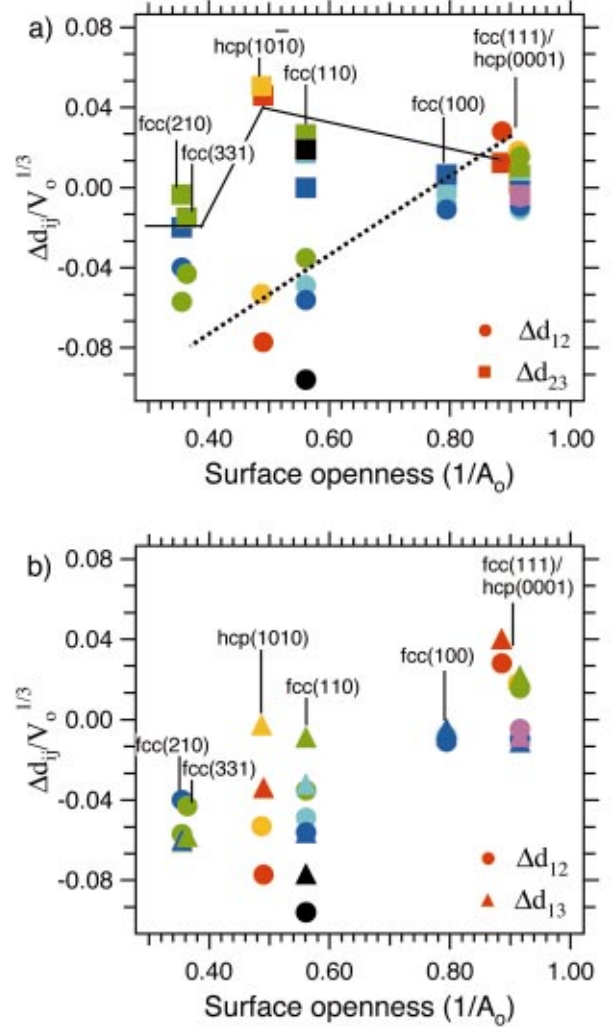


FIG. 6. (Color) Measured static interplanar relaxation. d_{12} (circles) and d_{23} (squares) are displayed in (a) and d_{12} and d_{13} in (b). The color code is shown in Fig. 5(a). The references for data points are the same as those in Fig. 5, except: Cu(110) (Ref. 38), Cu(210) (Ref. 39), Al(210) (Ref. 40), Ni(100) (Ref. 41), Ni(110) (Ref. 42), Pb(110) (Ref. 43), Al(331) (Ref. 44).

for the fcc(110) surfaces, is more general. The major unresolved question is still the same. Why does the second plane do what it does?

IV. DISCUSSIONS

The picture developed by Narasimhan for fcc(110) surfaces¹⁰ can be extended to include more open surfaces and to explain why *sp*-bonded metals show a different thermal behavior in α_{12} . The conclusion of this calculation was that for the relaxed static structure of the surface there was a dramatic enhancement in the nearest-neighbor force constant between the surface atom and the atom below in the third plane.¹⁰ This renormalization of the force constants resulted in an enhancement of the thermal vibrations parallel to the surface and a reduction in the vibrational amplitude perpen-

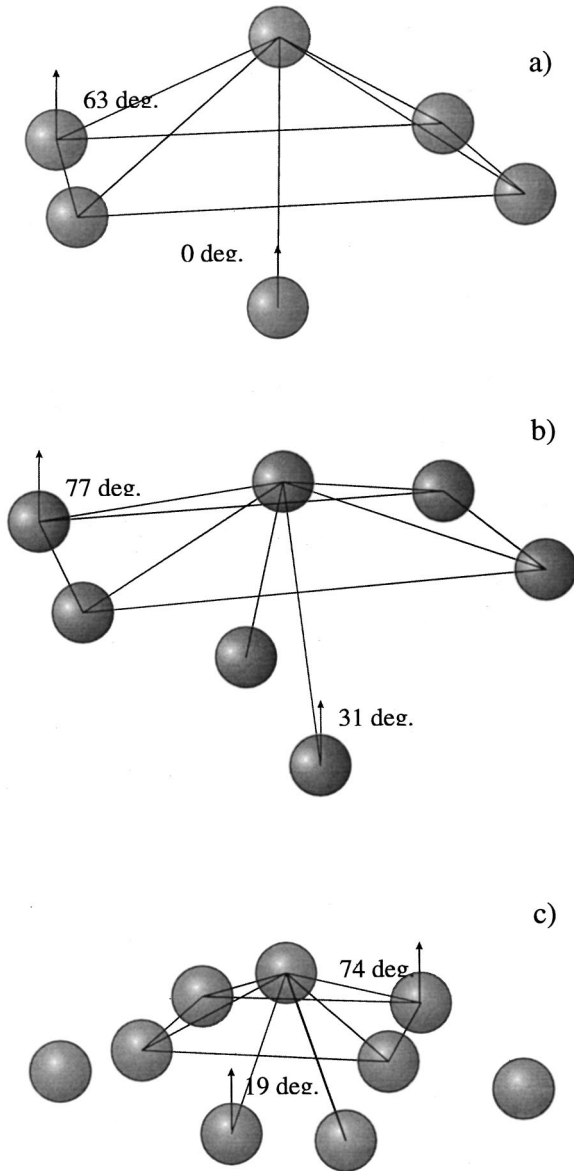


FIG. 7. Marble model of nearest-neighbor configuration for different surfaces: (a) fcc(110), (b) hcp(10 $\bar{1}$ 0), (c) fcc(210).

dicular to the surface. The rigid force constants between planes one and three allow only a small thermal expansion in d_{13} , however, the vibration of atoms in the second layer can be soft because the force constant between the first and the second interlayer is smaller than that between the first and third layer¹⁰. *It was this enhanced parallel motion, not the anharmonicity in the interplanar potential that led to thermal expansion or contraction.*

The geometrical structure at surfaces provides the first contribution to this picture by reducing the relative vibrational amplitudes normal to the surface. Figure 7(a) shows the nearest-neighbor (NN) configuration for a surface atom at a fcc(110) surface. It is quite easy to rationalize the results of Narasimhan.¹⁰ As she correctly pointed out, the change in the bond length does not scale with the change in d_{12} and d_{13} because of the bond angles. For example, for the $T=110$ K structure of Cu(110) there is a 4.8% contraction in the 1-3

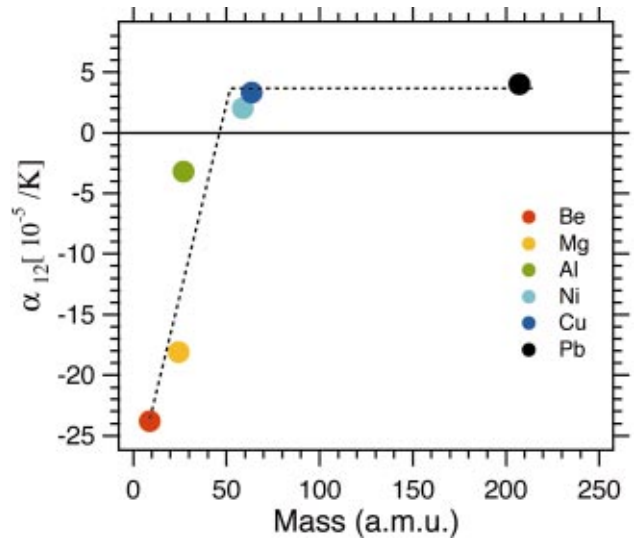


FIG. 8. (Color) Surface thermal expansion coefficient in the first interlayer α_{12} as a function of the mass of the atom in the crystal for all of the open faces data displayed in Fig. 5(a).

bond length but only a 2.4% contraction in 1-2 bond length; while the change in d_{12} and d_{13} are -10% and -5% , respectively.³⁸ If we assume the change of the force constant is proportional to the change in the bond length, then the force constant perpendicular to the surface between the first and third planes is larger than that between the first and second planes, which is confirmed by calculations.¹⁰ Now we can apply this idea to the other open faces. Figure 7(b) shows the NN structure for the relaxed hcp(10 $\bar{1}$ 0) surface. There are four bonds between the surface atom and the atoms in the second plane but the angle is very large (77°) indicating that changes in d_{12} will have little effect on the force constant in this simple model. But there are two NN atoms in the third layer with an angle of 31° with respect to the surface normal. Again, by assuming that the change of the force constant is proportional to the change in the bond length, on this surface the change in the first and third layers is $\sim 1.7\Delta d_{13} \times d^{\text{bulk}}$ which is larger than what would be expected for the fcc(110) surface ($\sim 1.0\Delta d_{13} \times d^{\text{bulk}}$). This model can be applied to even more open surfaces such as at the fcc(210). Figure 7(c) shows the NN atom configuration a fcc(210) surface. Here there are four NN atoms to a surface atom in the second plane at an angle of 74° . There are no NN atoms in the third plane and two in the fourth plane at an angle of 19° . Therefore we would predict that the increase in the force constant between the atom in the first layer with the NNs in the fourth would be $\sim 1.9\Delta d_{14} \times d^{\text{bulk}}$. For these more open surfaces the Narasimhan model has to be extended to talk about enhancement in the force constant between the first and fourth layers.

This geometrical picture would indicate that Cu(110) should show the same thermal behavior as Al(110) but it does not. Vibrational amplitudes depend also on mass. In an attempt to elucidate the influence of mass, Fig. 8 displays the dependence of the first interplanar thermal expansion coefficient α_{12} as a function of atomic mass for open face materials. Thermal contraction in the first interlayer spacing occurs

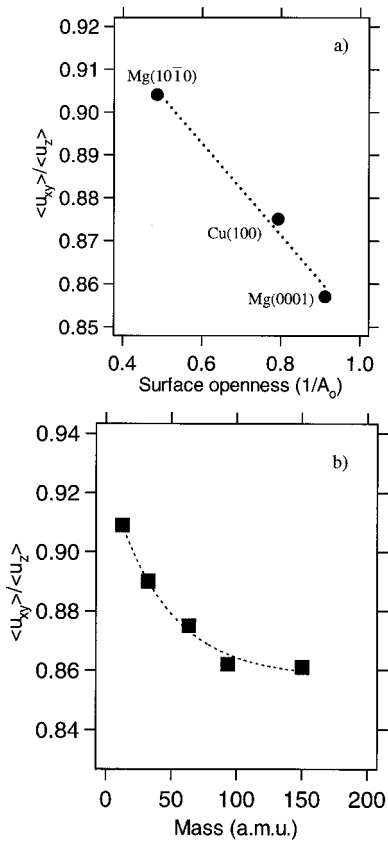


FIG. 9. (a) Calculated ratio of MSDs parallel to and perpendicular to the surface against surface openness at $T=100$ K for Mg(0001) by using 56 layer slabs with seven nearest-neighbor bulk force constants, Cu(100) by using 30 layer slabs with four nearest-neighbor bulk force constants, and Mg(10T0) by using 54 layer slabs with seven nearest-neighbor bulk force constants. (b) Calculated ratio of MSDs parallel to and perpendicular to the surface as a function of mass for a fcc(100) structure by using 30 layer slabs with four nearest-neighbor bulk force constants (taken for Cu) at $T=100$ K.

experimentally only for light mass materials where the mass is less than 50 amu. For masses greater than 50, the thermal expansion is always positive. Following Narasimhan's suggestion¹⁰ that what is important is the enhancement of the vibrational amplitude parallel to the surface compared to perpendicular to the surface, model calculations have been performed. A simple slab calculation of the mean-squared displacements (MSDs) was conducted using bulk force constants for Mg(0001), Cu(100), and Mg(10T0) at $T=100$ K. Figure 9(a) shows the results of the ratio of the MSDs parallel ($\langle u_{xy} \rangle$) to and perpendicular ($\langle u_x \rangle$) to the surface for these three surfaces, showing a linear dependence upon $1/A_o$. The more open the surface is, the larger is the ratio between the MSDs parallel and perpendicular to the surface, which as suggested by Narasimhan leads to large thermal expansion or contraction. This simple model can be used to explore the effect of mass on the ratio of the MSDs parallel to and perpendicular to the surface. Figure 9(b) shows the results for a fcc(100) surface at $T=100$ K with the force constants for Cu. Indeed, the ratio of in-plane vibra-

tions to perpendicular vibrations is related to the mass, where as the mass becomes smaller the ratio between the MSD parallel and perpendicular to the surface becomes larger. This very simple model violates our cardinal rule by not including changes in the force constants between different planes, which is a consequence of the interplanar relaxation, but the model calculation does show that the mass of the atoms in the surface can account for experimental trends. More sophisticated calculations are needed to confirm or reject the ideas presented here.

V. CONCLUSIONS

A picture is emerging of the basic physics associated with the thermal properties of metal surfaces that now can be tested with sophisticated calculations. The creation of a surface breaks the translational symmetry of the bulk causing a rearrangement of the charge and the atomic structure. This static rearrangement results in a renormalized of the force constants at the surface, and consequently, significantly different thermal vibrations. For the open surface, the most important effect is the enhanced bonding (force constant) between NN atoms in the first plane and directly below in the third plane for fcc(110) or hcp(10T0), and fourth planes for fcc(210) or fcc(331). This results in an enhancement in the vibrational amplitude of the surface atoms parallel to the surface and a reduction in their motion perpendicular to the surface. The impact of this enhancement on thermal expansion depends on the atomic mass, with lighter atoms showing greater effects. In all cases where quantitative calculations have been performed, the interplanar potentials do not display significant anharmonicity, so in this region of broken symmetry, thermal expansion or contraction occurs without anharmonicity.

It appears that a general understanding of the thermal properties of metal surfaces is eminent, changing fundamentally what is described as "common sense." Narasimhan's calculations for fcc(110) surface¹⁰ can obviously be extended to surfaces of different bulk crystal structure and to other faces. The missing ingredient is an understanding of why these changes in surface force constants can produce thermal expansion in d_{12} in some metals and contraction in others. Since the static interplanar relaxation is so important, the community needs to revisit the question raised by Feibelman. Does first principles theory really work for reactive transition metal surfaces.⁸

ACKNOWLEDGMENTS

We would like to thank M.A. Van Hove and A. Barbieri for computer LEED codes, J.B. Hannon for computer codes of slab calculations, and A. Thesen for helping in the experiment. This work was supported by the National Science Foundation Grant No. DMR-0105232 and Oak Ridge National Laboratory, managed by UT-Battelle, LLC, for the U.S. Dept. of Energy under Contract No. DE-AC05-00OR22725. One of us (Ph. H.) was supported by the Danish National Research Council.

- ¹R. Smoluchowski, Phys. Rev. **60**, 661 (1941).
- ²M. W. Finnis and V. Heine, J. Phys. F: Met. Phys. **4**, L37 (1974).
- ³N. D. Lang and W. Kohn, Phys. Rev. B **1**, 4555 (1970).
- ⁴K. Pohl, Ph.D. thesis, University of Pennsylvania, 1997.
- ⁵Ph. Hofmann, K. Pohl, R. Stumpf, and E. W. Plummer, Phys. Rev. B **53**, 13 715 (1996).
- ⁶U. Landman, R. N. Hill, and M. Mostoller, Phys. Rev. B **21**, 448 (1980); R. N. Barnett, U. Landman, and C. L. Cleveland, *ibid.* **28**, 1685 (1983); P. Jiang, P. M. Marcus, and F. Jona, Solid State Commun. **59**, 275 (1986); J.-H. Cho, Ismail, Z. Zhang, and E. W. Plummer, Phys. Rev. B **59**, 1677 (1999); Pavlin Staikov and Talat S. Rahman, *ibid.* **60**, 15 613 (1999).
- ⁷P. J. Feibelman, Phys. Rev. B **53**, 13 740 (1996).
- ⁸P. J. Feibelman, Surf. Sci. **360**, 297 (1996).
- ⁹A. P. Baddorf, V. Jahns, D. M. Zehner, H. Zajonz, and D. Gibbs, Surf. Sci. **498**, 74 (2002).
- ¹⁰S. Narasimhan, Phys. Rev. B **64**, 125409 (2001).
- ¹¹K. Pohl, J.-H. Cho, K. Terakura, M. Scheffler, and E. W. Plummer, Phys. Rev. Lett. **80**, 2853 (1998).
- ¹²H. Göbel and P. V. Blanckenhagen, Phys. Rev. B **47**, 2378 (1993).
- ¹³Ismail, E. W. Plummer, M. Lazzeri, and S. de Gironcoli, Phys. Rev. B **63**, 233401 (2001).
- ¹⁴G. Helgesen, D. Gibbs, A. P. Baddorf, D. M. Zehner, and S. G. J. Mochrie, Phys. Rev. **48**, 15 320 (1993).
- ¹⁵B. W. Busch and T. Gustafsson, Surf. Sci. **407**, 7 (1998).
- ¹⁶N. Marzari, D. Vanderbilt, A. De Vita, and M. C. Payne, Phys. Rev. Lett. **82**, 3296 (1999).
- ¹⁷S. Narasimhan and M. Scheffler, Z. Phys. Chem. (Munich) **202**, 253 (1997).
- ¹⁸M. Lazzeri and Stefano de Gironcoli, Phys. Rev. Lett. **81**, 2096 (1998).
- ¹⁹A. Baraldi, S. Lizzit, K. Pohl, Ph. Hofmann, and Stefano de Gironcoli (unpublished).
- ²⁰A. Mikkelsen, J. Jiruse, and D. L. Adams, Phys. Rev. B **60**, 7796 (1999).
- ²¹J. P. Toennies and Ch. Wöll, Phys. Rev. B **36**, 4475 (1987).
- ²²K. M. Ho and K. P. Bohnen, Phys. Rev. Lett. **56**, 934 (1987).
- ²³A. M. Raphuthi, X. Q. Wang, F. Ercolessi, and J. B. Adams, Phys. Rev. B **52**, R5554 (1995).
- ²⁴J. B. Pendry, J. Phys. C **13**, 937 (1980).
- ²⁵M. A. Van Hove and A. Barbiere (unpublished).
- ²⁶*International Tables for X-Ray Crystallography* (Kynoch, Birmingham, England, 1962), Vol. III; Y. S. Touloukian, R. K. Kirby, R. E. Taylor, and P. D. Desai, *Thermal Expansion: Metallic Elements and Alloys*, Thermophysical Properties of Matter Vol. 12 (IFI/Plenum, New York, 1970).
- ²⁷M. Lazzeri, Ph.D. thesis, SISSA, Italy, 1999; M. Lazzeri and Stefano de Gironcoli, Phys. Rev. B **65**, 245402 (2002).
- ²⁸P. T. Sprunger, K. Pohl, H. L. Davis, and E. W. Plummer, Surf. Sci. **297**, L48 (1993).
- ²⁹Alan F. Wright, P. J. Feibelman, and Susan R. Atlas, Surf. Sci. **302**, 215 (1994); Pavlin Staikov and Talat S. Rahman, Phys. Rev. B **60**, 15 613 (1999); Ismail, Ph. Hofmann, E. W. Plummer, Claudia Bungaro, and W. Kress, *ibid.* **62**, 17 012 (2000).
- ³⁰J. R. Noonan and H. L. Davis, J. Vac. Sci. Technol. A **8**, 2671 (1990).
- ³¹P. Statiris, H. C. Lu, and T. Gustafsson, Phys. Rev. Lett. **72**, 3574 (1994).
- ³²K. H. Chae, H. C. Lu, and T. Gustafsson, Phys. Rev. B **54**, 14 082 (1996).
- ³³H. C. Lu, E. P. Gusev, E. Garfunkel, and T. Gustafsson, Surf. Sci. **352**, 21 (1996).
- ³⁴A. P. Baddorf, V. Jahns, D. M. Zehner, H. Zajonz, and D. Gibbs, Surf. Sci. **498**, 74 (2002).
- ³⁵Y. Cao and E. Conrad, Phys. Rev. Lett. **65**, 2808 (1990).
- ³⁶J. W. M. Frenken, F. Hussien, and J. F. van der Veen, Phys. Rev. Lett. **58**, 401 (1987).
- ³⁷Y. Cao and E. Conrad, Phys. Rev. Lett. **64**, 447 (1990).
- ³⁸H. L. Davis, J. R. Noonan, and L. H. Jenkins, Surf. Sci. **83**, 559 (1979).
- ³⁹Ismail, S. Chandravakar, and D. M. Zehner, Surf. Sci. **504**, L201 (2002).
- ⁴⁰D. L. Adams, V. Jensen, X. F. Sun, and J. H. Vollesen, Phys. Rev. B **38**, 7913 (1988).
- ⁴¹W. Old, H. Lindner, U. Starke, K. Heinz, and K. Muller, Surf. Sci. **224**, 179 (1989).
- ⁴²D. L. Adams, L. E. Petersen, and C. S. Sorensen, J. Phys. C **18**, 1753 (1985).
- ⁴³U. Breuer, K. C. Prince, H. P. Bonzel, W. Old, K. Heinz, and K. Muller, Surf. Sci. **239**, L493 (1990).
- ⁴⁴D. L. Adams and C. S. Sorensen, Surf. Sci. **166**, 495 (1986).